

Crack propagation and toughening mechanism of bilayered short-fiber reinforced resin composite structure - evaluation up to six months storage in water

Journal:	<i>Dental Materials Journal</i>
Manuscript ID	DMJ2021-321.R2
Manuscript Type:	Original paper
Date Submitted by the Author:	n/a
Complete List of Authors:	Bijelic-Donova, Jasmina; University of Turku Institute of Dentistry, Department of Prosthetic Dentistry and Stomatognathic Physiology Garoushi, Sufyan; University of Turku Institute of Dentistry, Department of Biomaterials Science Lassila, Lippo; University of Turku Institute of Dentistry, Department of Biomaterials Science Rocca, GT; University of Geneva Faculty of Medicine, School of Dentistry, Division of Cariology and Endodontology Vallittu, Pekka; University of Turku Institute of Dentistry, Department of Biomaterials Science and City of Turku Welfare Division
Keywords:	Bilayered composite restoration, Discontinuous fibers, Fracture path, Fracture toughness, Load curve
Categories:	Composite resin < Primary Research Field (Sub Field), Testing method < Primary Research Field (Sub Field)

SCHOLARONE™
Manuscripts

Original paper

Crack propagation and toughening mechanism of bilayered short-fiber reinforced resin composite structure - evaluation up to six months storage in water

Jasmina BIJELIC-DONOVA^{1*}, Sufyan GAROUSHI², Lippo VJ LASSILA², Giovanni Tommaso ROCCA³, Pekka K VALLITTU^{2,4}

¹ Department of Prosthetic Dentistry and Stomatognathic Physiology, Institute of Dentistry, University of Turku, Lemminkäisenkatu 2, Turku, Finland

² Department of Biomaterials Science, Institute of Dentistry, University of Turku, Itäinen pitkätie 2, Turku, Finland

³ Division of Cariology and Endodontology, School of Dentistry, University of Geneva, 19, rue Lombard, 1205 Genève, Switzerland

⁴ City of Turku Welfare Division, Oral Health Care, Lemminkäisenkatu 2, Turku, Finland

Key words: Bilayered composite restoration, Discontinuous fibers, Fracture path, Fracture toughness, Load curve.

Number of reprints: 50

* Corresponding author:

Dr. Jasmina Bijelic-Donova

Department of Prosthetic Dentistry and Stomatognathic Physiology

Institute of Dentistry, University of Turku

Lemminkäisenkatu 2, 3rd floor

20520 Turku, Finland

e-mail: jabije@utu.fi

ABSTRACT

Clinically relevant parameters, such as stress intensity factor of bilayered resin composite structure with short fiber base and its stability over time, has yet to be investigated. This study investigated the stress intensity factor of pre-cracked bilayered specimens composed of short fiber resin composite base (SFC) and particulate filler resin composite (PFC) as veneering layer, with a crack located in the PFC layer, 0.5 mm away from the PFC-SFC interface. Monolayered specimens served as controls. All specimens were stored in water at 37°C either for 1 week, 1 month or 6 months before testing. Two-way ANOVA ($p=0.05$) was used to determine the differences among the groups. Results indicated that SFC base improve the brittleness of the PFC. The type of short fibers affected the crack propagation; fiber bridging in millimeter-scale SFC was the main crack arresting mechanism, whereas fiber pulling observed in micrometer-scale SFC mainly deviated the crack path.

Key words: Bilayered composite restoration, Discontinuous fibers, Fracture path, Fracture toughness, Load curve.

INTRODUCTION

Clinical use of direct particulate filler composites (PFCs) has been extended to large and cusp replacing restorations¹⁻³), with satisfactory results⁴). Direct posterior PFC restorations fail predominantly as a result of fracture of the material, so called technical failure, either a superficial chipping or bulk (cohesive) material fracture. Usually, chippings are associated with errors in placement technique or inadequate manipulation of the material and occur earlier than cohesive fractures, which are considered as late failures associated with material deterioration over time⁵). In order to minimize the incidence of these failures, recommendations for placement techniques have been made⁶). From a purely technical procedure oriented perspective^{2,3,7}), progress has expanded towards restorative techniques utilizing combinations of restorative materials in order to enhance the endurance of large direct PFC restorations and prevent catastrophic fractures.

One such restorative technique is the bilayered technique, where a fiber-reinforced composite (FRC), usually a continuous prepreg (often bidirectional, *i.e.* fiber net) is placed at the cavity bottom as a crack stopping layer⁸⁻¹¹). For the same purpose, however, nowadays available are also various discontinuous-FRC systems, so called short-fiber reinforced composites (SFCs), where short fibers are embedded in the resin composite and ready to be used in a conventional composite-like manner¹²⁻¹⁴). The fiber-reinforced restoration is finished by veneering it with a capping layer of PFC, in order to enhance the esthetic appearance, because exposed fibers increase the surface roughness¹⁵) and could be inhaled¹⁶). From structural point of view, the presence of different material components in a restoration makes the system heterogeneous and the final restoration would exhibit different properties than its individual material components¹⁷⁻¹⁹). Consequently, the endurance of a bilayered composite structure would depend on the types of both materials (FRC or SFC and PFC) used and the thickness ratio of fiber structure versus veneering layer^{17,18,20,21}). However,

this might be challenging to test clinically. An *in vitro* test that closely resembles the clinical behavior of a material is the fracture toughness test. The fracture toughness is characterized by the critical stress intensity factor (K_{IC}) around a crack tip in a pre-cracked structures and is used when the goal is to assess the ability of the material containing a flaw to resist unfavorable fracture^{22–24}). In addition, this material property has a positive correlation with clinical fractures of restorative materials²⁵).

Therefore, the aim of this study was to assess the stress intensity factor around the crack tip within a bilayered resin composite structure composed of SFC base covered with a surface PFC layer, which mimics the clinical application of the material^{13,26}). The effect of millimeter or micrometer scale SFC inclusion and six months storage in water on the stress intensity factor was also assessed. The crack was initiated in the PFC layer. Hence, in addition, the crack propagation towards the fiber base and inside the fiber layer was also analyzed by means of scanning electron microscopy (SEM). The hypotheses tested were that there would be 1) no difference in the stress intensity factor and toughening mechanisms between the two monolayered types of SFC; 2) a difference in the stress intensity factor between bilayered and monolayered composite structures and 3) no effect of the water storage on the stress intensity factor of tested materials and structures.

MATERIALS AND METHODS

Study materials and terminology

The materials used in this study are listed in Table 1 and groups are described in Table 2. Pre-cracked bending bars (PCBB) of 2.5mm x 5mm x 25 mm were prepared to evaluate the critical stress intensity factor (K_{IC}) around the crack tip within monolayered and bilayered resin composite specimens. For monolayered structures, the method is known as single-edge-notched-beam (SENB) adapted to the ISO 20795-2 standard, used to determine the fracture

toughness (FT) property of the material (K_{IC} same as FT). As this method has been developed for evaluating the fracture toughness of single material only (*i.e.* monolayer, monolithic), the same terminology cannot be used for bilayered (bimaterial) structures. Hence, the term stress intensity factor (KI, found in literature also as K; KI same as K) is used in this study for bilayered specimens. A total of 150 pre-cracked bending bars ($n=10/\text{group}$) were prepared and divided into five groups with three different storage times each (Table 2). Monolayered and bilayered specimens were fabricated using a mold with a centrally located prefabricated slot extending to half of its depth. This allowed the fabrication of specimens with a precisely fabricated notch at the midline of the specimen length and a standardized crack depth of 2.5 mm. The monolayered specimens were prepared from plain SFCs and PFC, and were used as controls (Table 2). Bilayered specimens were prepared from two different SFC types, everX Posterior (EXP) (GC, Leuven, Belgium) and everX Flow, dentin shade (EXFD) (GC), in a combination with a conventional PFC (G-aenial Posterior (GP), shade A2) (GC) (Table 2). The thickness of the SFC layer was 2 mm and the remaining 3 mm was the thickness of the PFC. The pre-fabricated crack was created in the PFC layer (Fig. 1).

Fracture toughness and stress intensity factor measurement

The custom-made split mold was placed on a Mylar-strip-covered glass. For the bilayered specimens, the SFC was first extruded to height of 2 mm, pressed and light-cured in five overlapping portions, 20 s each. The remaining thickness of 3 mm was then filled with the PFC. In order to secure standardized dimensions of the layers, the inner side of the mold was marked at depth of 2 mm and upon polymerization of the SFC layer, the thickness of the remaining half (3 mm) was measured with a digital caliper. Before light-curing the PFC layer, a sharp and centrally located crack was produced by inserting a straight edged razor blade into the prefabricated slot. Then, Mylar-strip-covered glass slabs were pressed firmly

on top of the mold on each side of the blade to ensure even distribution of the surface PFC material around the steel blade before polymerization. Upon the removal from the mold, each specimen was also light-cured on the opposite side. The light-curing of all composites was performed in five overlapping portions, 20 s each. An LED light-curing unit (Elipar S10, 3M ESPE, St. Paul, MN, USA) with a calibrated (MARC® Resin, BlueLight analytics Inc., Halifax, Canada) light intensity of 1200 mW/cm² was used throughout this study. The tip of the light curing unit was in approximate contact with the mold. For monolayered specimens, the restorative material was inserted into the mold placed in 2 increments, each of approximately 2.5 mm in thickness. Each layer was light-cured for 20 s in five separate overlapping portions. Immediately upon preparation, the notch in all specimens was sharpened by sawing the notch with a sharp razor blade, in order to ensure that tip of the notch is sharp and to secure the creation of the pre-crack in the polymerized material. Otherwise, creating the notch by layering the composite material around the razor blade would not fulfill the critical assumption of having a true pre-crack. The thickness of the layers in the bilayered specimens and the location of the crack were analyzed under a light-microscope (Leica, Wild, Heerbrugg, Switzerland). All specimens were stored in water at 37°C either for 1 week, 1 month or 6 months before testing. The specimens were tested in three-point bending mode, in a universal material testing machine (Model LRX, Lloyd Instruments Ltd., Fareham, England) at a crosshead speed of 1.0 mm/min. The SFC layer was facing the compression side, that is, being in contact with the cylindrical loading tip (2 mm diameter). Loading data were computed using PC software (Nexygen, Lloyd Instruments Ltd., Fareham, England). Force-displacement curves were monitored and documented.

The stress intensity factor (KI) was calculated using the equation $KI = [P L/B W^{3/2}] f(x)$, where: $f(x) = 3/2x^{1/2} [1.99-x(1-x) (2.15-3.93x+2.7x^2)] / (1+2) (1-x)^{3/2}$ and $0 < x < 1$ with $x=a/W$. Here, **P** is the maximum load in kilonewtons (kN), **L** is the span length (2 cm),

B is the specimen thickness in centimeters (cm), **W** is the specimen width (depth) in cm, **x** is a geometrical function dependent on a/W , and **a** is the crack length in cm. Work of fracture (W_f) (the energy required to fracture the specimen) was calculated from the area under the load-displacement curve of the specimens and reported in units of Ncm.

Scanning electron microscopy observation

Scanning electron microscopy (SEM, JSM 5500, Jeol Ltd., Tokyo, Japan) provided the fractographic examination of the specimens. Three fractured specimens from each group were gold sputter coated (BAL-TEC SCD 050 Sputter Coater, Balzers, Liechtenstein) before the SEM examination.

Statistical analysis

The data were analyzed using SPSS version 23 (SPSS, IBM Corp., Armonk, New York, USA) using analysis of variance (ANOVA) followed by a Tukey HSD post hoc test. Two-way ANOVA ($p=0.05$) was used to determine the differences among the groups. The dependent factor was the fracture toughness or work of fracture, whereas the independent factors were the material and storage condition.

RESULTS

The stress intensity factor (Fig. 2) between monolayered SFC types (EXP and EXFD) as well as between the bilayered structures (EXP-GP and EXFD-GP) was comparable regardless of the storage time in water ($p>0.05$). The KI difference among monolayered SFCs and monolayered PFC was statistically significant ($p<0.05$), as well as the difference among monolayered SFCs and bilayered composite structures ($p<0.05$). On the other hand, the KI difference among monolayered PFC and both bilayered composite structures was not

statistically significant ($p > 0.05$) after one week of water storage. However, at one month and six months of storage in water, EXFD-GP was similar ($p > 0.05$) to the monolayered PFC whereas the stress intensity factor of EXP-GP was significantly higher than the monolayered PFC ($p < 0.05$).

Likewise, the work of fracture (Fig. 3) between the monolayered SFCs was comparable ($p > 0.05$) and statistically different to the rest of the groups ($p < 0.05$). EXFD values deteriorated in water significantly after six months ($p < 0.05$). The work of fracture for the monolayered PFC was statistically lower in comparison to the rest of the groups ($p < 0.05$). The difference between the bilayered composite structures was significant at the first week ($p < 0.05$), and it stabilized after one month and after six months ($p > 0.05$). The storage time did not affect the work of fracture ($p > 0.05$).

Upon failure, none of the EXP and one EXFD specimen broke into two halves. Bilayered specimens did not experience wedge opening either. Conversely, all GP specimens broke into two halves. SEM images of crack development in bilayered resin composite structures EXP-GP and EXFD-GP are shown in Figs. 4 and 5, respectively.

DISCUSSION

Various formulations of short-fiber reinforced systems have been developed with the aim of providing a user-friendly material that could overcome the weakness of conventional PFCs. Best known SFCs are Alert, Nulite F and Restolux, familiar also as micrometer scale (or low aspect ratio) short-fiber reinforced composite materials, which have shown somehow unsatisfactory clinical results¹⁴. The last one (Restolux) failed to achieve the wanted intentions and was withdrawn from the market.

Material development has progressed since the early 2000s and new types of SFCs have emerged. One study compared three and another five new brands of SFCs^{27,28}.

Alshabib *et al.* reported superior performance for the millimeter-scale SFC (everX Posterior)²⁷⁾ and Lassila *et al.* too, showed that this millimeter-scale SFC (everX Posterior) and also one micrometer-scale SFC (everX Flow) had better fracture toughness than other commercial SFCs (Alert, NovaPro-Flow, NovaPro-Fill, EasyCore, Build-It and TI-Core)²⁸⁾. Lately, interest has been focused on investigating the resistance curve behavior, essential work of fracture and interface interaction of these particular SFCs (everX Posterior and everX Flow) in both, monolayered and bilayered structures^{21,29-31)}. Consequently, selecting the SFC materials for the purposes of the present investigation was based on the results of these studies.

Clinical fracture of resin composite restorations is commonly preceded with a failure process containing events of crack initiation and progression, so called hindered cracks, that at the time of failure reach the catastrophic critical length. This study set-up was therefore designed to mimic a clinical condition where the initial failure crack is in the PFC portion of the PCBB specimen, which clinically simulates the veneering resin composite layer over the SFC base. For illustration, in a restored tooth unit, the cracks originate from the occlusal top surface (veneering resin composite layer in this study) and continue to the bulk of the restoration (SFC base in this study). Consequently, this scenario resulted in having bar specimens with the veneering composite layer (where the crack tip was located) in tension and SFC base in compression. The results of the stress intensity factor test indicated that both material type (SFC, PFC) and structure design (monolayer or bilayer) have influence on the intrinsic toughness. The stress intensity factor values between both monolayered SFCs (EXP and EXFD) as well as between both bilayered resin composite structures (EXP-GP and EXFD-GP) were comparable, but there was a difference to monolayered PFC (GP). However, only the bilayered structure composed of EXP-GP was statistically different to

monolayered PFC, while the bilayered structure composed of EXFD-GP was not. Therefore, the first null hypothesis was accepted and the second null hypothesis was partially rejected.

It should be reemphasized that *fracture toughness* term is used for specimens prepared from one material only (as control groups in this study), whereas the term *stress intensity factor* is used when specimens are made by layering two different materials. Subsequently, the stress intensity factor is defined for the crack being located in one of the two materials and depends on the elastic modulus ratio of the materials involved. It is significant for analyzing the crack propagation and arrest at the interface.

Consequently, the difference between the bilayered structures in this study could be explained by the fracture toughness mismatch between the materials composing the bilayered structure and by the difference in short fiber dimensions (diameter and length) of the SFCs. When the crack propagates from a material with lower to a material with higher fracture toughness (from PFC to SFC), it will arrest at the interface, due to the toughness mismatch at the interface. Thereafter, the material with higher toughness would absorb the stress. For everX Posterior, everX Flow and G-aenial Posterior respectively, fracture toughness values obtained in this study were 2.18, 2.05 and 0.78 MPa m^{1/2}. Similar explanation has been mentioned for matching versus mismatching flexural moduli of the materials composing a bilayered resin composite structure^{21,29}) and also, the same has been found to be a principle mechanism for crack arrest at DEJ (dentino-enamel-junction)³²). The main difference regarding the material composition of SFCs is the dimension of short fibers. The packable SFC (everX Posterior) contains 8.6 wt% of 0.3-1.9 mm long and 17 μm thick E-glass fibers^{30,33}), whereas the flowable SFC (everX Flow) contains 25 wt% of E-glass fibers 140-300 μm in length and 6-7 μm thick^{21,29}). The aspect ratio (l/d) for EXP could be as high as 112 and for EXFD about 30. The finding that the stress intensity factor of the bilayered structures was higher in comparison to the plain (control) PFC, reveals the action of the

reinforcing effect of the short fibers during fracture of the bilayered structure, which constitutes a PFC as one component (veneering layer) and SFC as another component (supporting base). This was the first conclusion of this study.

Force-displacement curves (Figs. 6-7) showed that the crack for monolayered PFC specimens was instantaneous. For SFCs, the first peak of the curve represents the event when the crack reaches the PFC-SFC interface (elastic range). In the plastic range, the crack propagates in the SFC layer. For EXP the curve increases more than for EXFD, which is more flat. Prior complete fracture (degradation region), the crack already slows down and at the break point is arrested by a fiber crossing or interfering with its direction.

Work of fracture is determined by the total fracture energy covering the whole area under the load-displacement curve. The work of fracture was higher for both SFCs than for the rest of the materials and their combinations, which is a sign that the fiber toughening mechanisms increase the total fracture energy. Additionally, it could also indicate that the fibers decrease the notch sensitivity and thus, require more energy to fracture. However, the work of fracture of EXP was more stable than that of EXFD, which deteriorated in water as a monolayer and as a bilayer material in comparison to EXP. The difference could be due to the different fracture toughening processes of the millimeter- and the micrometer short fibers. Packing (agglomeration) of micrometer short fibers is, in theory, easier to occur than for millimeter short fibers, and could affect the fracture mechanics. Agglomeration of short fibers, however, was not observed in this study and could not be further elaborated.

SEM analyses revealed differences in the path of crack propagation between the two SFC types (Figs. 4 and 5). The difference between the millimeter-scale (EXP) and micrometer-scale (EXFD) SFC is in the portion of bridging and pull out fibers. For EXP more bridging fibers were already observed at the opening. In the middle portion mainly bridging fibers and only some pull out were observed. At the end, there were more

perpendicularly orientated fibers. For the EXFD, partially pull out fibers at the opening were dominantly seen. In the middle portion, there were more pull out than bridging fibers, but some bridging was also present. Here multiple cracking of the matrix was also observed. At the end, there were more shorter fibers that were completely pulled out, and arrested the crack mainly by altering the crack path and consuming the energy.

From a fractographical point of view, fiber bridging in EXP effectively arrested the crack path, whereas fiber pulling observed in EXFD diverted the crack path. Hence, the retardation mechanism for EXFD is due to consuming the energy, not due to fiber orientation. Consequently, a second conclusion could be that fibers length and orientation in EXP was fractographically more favorable in arresting the fracture than in EXFD. For EXP with fewer but longer fibers, the bridging did not degrade at the crack tail, while for EXFD with more but shorter fibers, total fiber pull out was seen at the crack tail.

It is worth mentioning that, as elaborated in another study²¹⁾, the elastic fiber bridging, as in EXP, stores the strain energy in the fiber and causes residual energy over the debonded fiber length. The strain energy is desirable and the residual energy is undesirable for toughness **when the fiber degrades**. The fiber pull out, as in EXFD, creates a frictional energy in the pull out fiber length, which is desirable for toughness. These toughening mechanisms happen during the crack propagation and could explain why both SFCs had comparable toughness values regardless of the different short fiber lengths (millimeter and micrometer in EXP and EXFD, respectively) and the different crack arresting mechanisms.

The influence of water storage has been stated to be ultimately deleterious for fracture toughness³⁴⁾, but it shows some dependency upon composition and chemistry of the FRC material³⁵⁾. SFC systems as well, seem to be less influenced by water storage³⁰⁾. For PFCs, some stability could be expected after approximately two months³⁶⁾, however. On the other hand, water may also have some toughening capacity³⁷⁾. In the present study, the effect

of water storage was dependent on the storage time for the work of fracture, and on the material for the fracture toughness. An interaction between the water storage and the material was observed, and the overall effect was slightly deteriorating. Therefore, the third null hypothesis was partially accepted and results concur partially with the results of Tiu et al³⁰).

Factors, such as thickness of the veneering composite and stress distribution at the PFC-SFC interface, influence the fracture and failure properties. The thicker the SFC base layer, the greater the toughness²¹ and the load bearing capacity of the bilayered structure²⁰). Tiu *et al.* suggested applying the veneering composite in as thin layer as possible²¹), but the threshold thickness of this layer could be considered to be 2 mm²⁰). Thinner than a 2 mm layer of veneering composite concentrates the stress at the interface, however, 2 mm is optimal to avoid delamination and chipping²⁰). Thickness values in the present investigations were dictated by the pre-crack length (2,5 mm) which was intended to be placed in the PFC layer, but away from the PFC-SFC interface, in order to simulate a crack starting from the veneering resin composite layer and directed towards the SFC base. Hence, thickness values on 3 mm and 2 mm were selected for PFC and SFC layers respectively. In this way, the thickness of the veneering (PFC) layer was sufficient to fulfill the intended purpose and diminish the chances for chipping at the same time. The interface layer was not treated in any way, thus the beneficial effect of the oxygen inhibition layer at the adhesion interface was allowed³⁸).

Evaluation of KI for bilayered (bimaterials) structures could be questioned because of the simplification that has to be used for the calculation. This is one limitation of the study. Nonetheless, KI measurement for bimaterials is justified if both materials have isotropic properties and gradient free elastic moduli³²), as is also the case for resin composites. In this study, despite the simplification, values seem to be reasonable. Values measured for bilayered specimens are between monolayered PFC and monolayered SFC values suggesting

that approximation was acceptable. Other limitations are not having dry specimen groups and not measuring the water sorption.

Finally, this study is clinically relevant for designing and predicting the behavior of large restorations where a short-fiber base is utilized to support the tooth-restoration complex. These restorations are known as biomimetic. This study will aid clinicians in anticipating the future outcomes and treatments of such biomimetic restorations in terms of whether to repair (replace only the veneering part) or replace the whole restoration.

Lastly, the clinical relevance of the findings of the present investigation is that both SFC bases improved the brittleness of the PFC. However, deviation of the crack by EXFD is less expected than by EXP due to the very short fibers that tend to pull out, which means that EXFD reinforcement could also lead to unfavorable fracture modes. Possibly, this might be avoided by applying it in a thicker layer, as recently shown by other authors²¹).

CONCLUSIONS

Within the limitations of this investigation, it could be concluded that: 1. both SFC materials improved the toughness of the PFC, but EXP-GP was intrinsically tougher; 2. both SFCs showed comparable toughness values, but toughening mechanism was different; 3. fibers orientation in EXP as shown by SEM was more favorable in arresting the crack than in EXFD. For EXP with fewer but longer fibers, the bridging did not degrade at the crack tail, while for EXFD with more but shorter fibers, total fiber pull out was seen at the crack tail; and 4. fiber bridging in EXP is the principal crack arresting mechanism, whereas fiber pulling observed in EXFD diverted the crack path. The retardation mechanism for EXFD is due to consuming the energy, not due to fiber orientation.

CONFLICT OF INTERESTS

The authors report no conflicts of interests. Author Pekka K. Vallittu consults Stick Tech Ltd., a member of the GC Group in RD and training.

For Peer Review

REFERENCES

1. Deliperi S, Bardwell DN. Clinical evaluation of direct cuspal coverage with posterior composite resin restorations. *J Esthet Restor Dent*. 2006; 18:256–265.
2. Loomans B, Hilton T. Extended resin composite restorations: techniques and procedures. *Oper Dent*. 2016; 41:S58–67.
3. Opdam N, Skupien J, Kreulen C, Roeters J, Loomans B, Huysmans MD. Case Report: a predictable technique to establish occlusal contact in extensive direct composite resin restorations: the DSO-Technique. *Oper Dent*. 2016; 41:S96–108.
4. Frankenberger R, Reinelt C, Glatthöfer C, Krämer N. Clinical performance and SEM marginal quality of extended posterior resin composite restorations after 12 years. *Dent Mater*. 2020; 36:e217–228.
5. Hickel R, Manhart J. Longevity of restorations in posterior teeth and reasons for failure. *J Adhes Dent*. 2001; 3:45–64.
6. Deliperi S, Bardwell DN. An alternative method to reduce polymerization shrinkage in direct posterior composite restorations. *J Am Dent Assoc*. 2002; 133:1387–1398.
7. Denehy G, Cobb D. Impression matrix technique for cusp replacement using direct composite resin. *J Esthet Restor Dent*. 2004; 16:227–233.
8. Butterworth C, Ellakwa AE, Shortall A. Fibre-reinforced composites in restorative dentistry. *Dent Update*. 2003; 30:300–306.
9. Deliperi S. Direct fiber-reinforced composite restoration in an endodontically-treated molar: a three-year case report. *Oper Dent*. 2008; 33:209–214.
10. Deliperi S, Bardwell DN, Coiana C. Reconstruction of devital teeth using direct fiber-reinforced composite resins: a case report. *J Adhes Dent*. 2005; 7:165–171.
11. Rocca GT, Rizcalla N, Krejci I. Fiber-reinforced resin coating for endocrown preparations: a technical report. *Oper Dent*. 2013; 38:242–248.

12. Manhart J, Chen HY, Hickel R. The suitability of packable resin-based composites for posterior restorations. *J Am Dent Assoc.* 2001; 132:639–645.
13. Tanner J, Tolvanen M, Garoushi S, Säilynoja E. Clinical Evaluation of Fiber-Reinforced Composite Restorations in Posterior Teeth - Results of 2.5 Year Follow-up. *Open Dent J.* 2018; 12:476–485.
14. van Dijken JWV, Sunnegårdh-Grönberg K. Fiber-reinforced packable resin composites in Class II cavities. *J Dent.* 2006; 34:763–769.
15. Lassila LVJ, Garoushi S, Tanner J, Vallittu PK, Söderling E. Adherence of *Streptococcus mutans* to fiber-reinforced filling composite and conventional restorative materials. *Open Dent J.* 2009; 3:227–232.
16. Dodson RF, Atkinson MAL, Levin JL. Asbestos fiber length as related to potential pathogenicity: A critical review. *Am J Ind Med.* 2003; 44:291–297.
17. Garoushi S, Lassila LVJ, Tezvergil A, Vallittu PK. Static and fatigue compression test for particulate filler composite resin with fiber-reinforced composite substructure. *Dent Mater.* 2007; 23:17–23.
18. Garoushi S, Lassila LVJ, Tezvergil A, Vallittu PK. Load bearing capacity of fibre-reinforced and particulate filler composite resin combination. *J Dent.* 2006; 34:179–184.
19. Keulemans F, Palav P, Aboushelib MMN, van Dalen A, Kleverlaan CJ, Feilzer AJ. Fracture strength and fatigue resistance of dental resin-based composites. *Dent Mater.* 2009; 25:1433–1441.
20. Omran TA, Garoushi S, Lassila L, Shinya A, Vallittu PK. Bonding interface affects the load-bearing capacity of bilayered composites. *Dent Mater J.* 2019; 38:1002–1011.
21. Tiu J, Belli R, Lohbauer U. Thickness influence of veneering composites on fiber-reinforced systems. *Dent Mater.* 2021; 37:477–485.
22. Ilie N, Hilton TJ, Heintze SD, Hickel R, Watts DC, Silikas N, et al. Academy of Dental

- Materials guidance—Resin composites: Part I—Mechanical properties. *Dent Mater.* 2017; 33:880–894.
23. Soderholm K-J. Review of the fracture toughness approach. *Dent Mater.* 2010; 26:e63–77.
24. Zhu X-K, Joyce JA. Review of fracture toughness (G, K, J, CTOD, CTOA) testing and standardization. *Eng Fract Mech.* 2012; 85:1–46.
25. Heintze SD, Ilie N, Hickel R, Reis A, Loguercio A, Rousson V. Laboratory mechanical parameters of composite resins and their relation to fractures and wear in clinical trials—A systematic review. *Dent Mater.* 2017; 33:e101–114.
26. Bijelic-Donova J, Keulemans F, Vallittu PK, Lassila LVJ. Direct bilayered biomimetic composite restoration: The effect of a cusp-supporting short fiber-reinforced base design on the chewing fracture resistance and failure mode of molars with or without endodontic treatment. *J Mech Behav Biomed Mater.* 2020; 103:103554.
27. Alshabib A, Silikas N, Watts DC. Hardness and fracture toughness of resin-composite materials with and without fibers. *Dent Mater.* 2019; 35:1194–1203.
28. Lassila L, Keulemans F, Vallittu PK, Garoushi S. Characterization of restorative short-fiber reinforced dental composites. *Dent Mater J.* 2020; 39:992–999.
29. Tiu J, Belli R, Lohbauer U. Rising R-curves in particulate/fiber-reinforced resin composite layered systems. *J Mech Behav Biomed Mater.* 2020; 103:103537.
30. Tiu J, Belli R, Lohbauer U. R-curve behavior of a short-fiber reinforced resin composite after water storage. *J Mech Behav Biomed Mater.* 2020; 104:103674.
31. Wendler M, Belli R, Schachtner M, Amberger G, Petschelt A, Fey T, et al. Resistance curves of short-fiber reinforced methacrylate-based biomedical composites. *Eng Fract Mech.* 2018; 190:146–158.
32. Bechtle S, Fett T, Rizzi G, Habelitz S, Klocke A, Schneider GA. Crack arrest within teeth

at the dentinoenamel junction caused by elastic modulus mismatch. *Biomaterials*. 2010; 31:4238–4247.

33. Bijelic-Donova J, Garoushi S, Lassila LVJ, Keulemans F, Vallittu PK. Mechanical and structural characterization of discontinuous fiber-reinforced dental resin composite. *J Dent*. 2016; 52:70–78.

34. Ferracane JL, Berge HX, Condon JR. In vitro aging of dental composites in water-Effect of degree of conversion, filler volume, and filler/matrix coupling. *J Biomed Mater Res*. 1998; 42:465-472.

35. Chai J, Takahashi Y, Hisama K, Shimizu H. Effect of Water Storage on the Flexural Properties Glass Fiber–Reinforced Composites. *Int J Prosthodont*. 2005; 18:28-33.

36. Alrahlah A, Silikas N, Watts DC. Hygroscopic expansion kinetics of dental resin-composites. *Dent Mater*. 2014; 30:143–148.

37. Lohbauer U, Frankenberger R, Krämer N, Petschelt A. Time-dependent strength and fatigue resistance of dental direct restorative materials. *J Mater Sci Mater Med*. 2003; 14:1047–1053.

38. Bijelic-Donova J, Garoushi S, Lassila LVJ, Vallittu PK. Oxygen inhibition layer of composite resins: effects of layer thickness and surface layer treatment on the interlayer bond strength. *Eur J Oral Sci*. 2015; 123:53–60.

FIGURE CAPTIONS

Fig. 1. Pre-cracked bending bar (PCBB) of 2.5mm x 5mm x 25 mm used to evaluate the stress intensity factor. PFC: particulate filler composite; SFC: short-fiber reinforced composite.

Fig. 2. Diagram showing the stress intensity factor (KI) values. EXP: everX Posterior; EXFD: everX Flow, dentin shade; GP: G-ænial Posterior. The horizontal lines and asterisk above the columns indicate statistically similar groups ($p>0.05$).

Fig. 3. Diagram showing the work of fracture (Wf) values. EXP: everX Posterior; EXFD: everX Flow, dentin shade; GP: G-ænial Posterior. The horizontal lines and the same letter or sign above the columns indicate statistically similar groups ($p>0.05$).

Fig. 4. SEM images of a crack through a bilayered EXP-GP specimen. A: showing the whole crack path length starting in the GP layer reaching the EXP-GP interface and continuing in the EXP layer. There is interface shearing and cracking when the crack opens. From here, the crack propagates along the path with least resistance towards the SFC layer; B: beginning part of the crack path in the SFC layer showing the crack opening with fiber bridging and partially fiber pull out; C: middle part of the crack path showing bridging fibers; D & E: final part of the crack path (crack tip) showing arrested crack by multiple short fiber(s). EXP: everX Posterior and GP: G-ænial Posterior.

Fig. 5. SEM images of a crack through a bilayered EXFD-GP specimen. A & B: showing the EXFD part of the fractured surface showing partially and totally pulled out fibers; C: middle part of the crack path with partial fiber pull out and D: final part of the crack path (crack tip) where the crack is intersected by single short fiber. EXFD: everX Flow, dentin shade and GP: G-ænial Posterior.

Fig. 6. Force-displacement curves for the investigated materials. Monolayered structures: EXP: everX Posterior; EXFD: everX Flow, dentin shade; GP: G-ænial Posterior, and Bilayered structures: EXP-GP: everX Posterior and G-ænial Posterior, and EXFD-GP: everX Flow, dentin shade and G-ænial Posterior. Extension from preload is same as displacement.

Figs. 7 a and b. Force-displacement curve for bilayered SFC-PFC structures accompanied with corresponding SEM photos at each range. The first peak in the curve represents the event when the crack reaches the PFC-SFC interface (elastic range). At this time the crack opens and fiber pull out begins to happen. After this, follows a drop until the crack finds the path with smallest resistance to the SFC layer. Here, fibers begin to carry the load and curve continues to increase (plastic range). In the plastic range, the crack propagates in the SFC layer. For EXP the curve increases more than for EXFD, which is more flat. During crack propagation, multiple cracking and crack deflection accompanied with simultaneous crack bridging, fiber pull out and matrix cracking take place (plastic range). These events consume the energy and crack begins to retard. Prior complete fracture (degradation region), the crack is already slowing down and at the break point is arrested by a fiber crossing or interfering with its direction. PFC-SFC: particulate filler composite - short-fiber reinforced composite bilayered structure. SFC: short-fiber reinforced composite, which are EXP: everX Posterior and EXFD: everX Flow, dentin shade. PFC: particulate filler composite, which is the GP: G-ænial Posterior. Extension from preload is same as displacement.



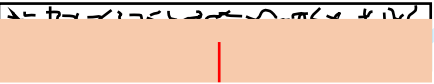
Table 1 The materials used and their composition

Material and Manufacturer	Type	Composition
G-aenial Posterior GC Corp, Tokyo, Japan	Packable PFC	UDMA, dimethacrylate co-monomers, pre-polymerized silica and strontium fluoride containing fillers 77 wt%, 65 vol%
everX Flow (dentin shade) GC Corp, Tokyo, Japan	Flowable SFC	Bis-EMA, TEGDMA, UDMA, micrometer scale glass fiber filler, Barium glass 70 wt%, 46 vol%
everX Posterior GC Corp, Tokyo, Japan	Packable SFC	Bis-GMA, PMMA, TEGDMA, millimeter scale glass fiber filler, Barium glass 76 wt%, 57 vol%

Bis-GMA, bisphenol-A-glycidyl dimethacrylate; UDMA, urethane dimethacrylate; TEGDMA, triethylene glycol dimethacrylate; Bis-EMA, Ethoxylated bisphenol-A-dimethacrylate; PMMA, polymethylmethacrylate; PFC: particulate filler composite; SFC: short-fiber reinforced composite resin; wt%, weight percentage; vol%, volume percentage.

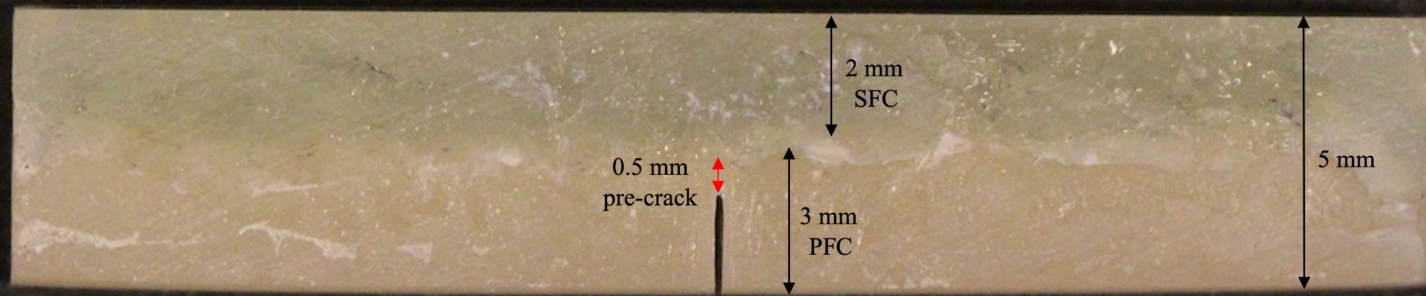
For Peer Review

Table 2 Designed groups

	Groups (n=10/group)	Abbreviations	Storage time
Monolayered specimens (n=90) Plain PFC (GP) 	EverX Posterior	EXP	1 week, 1 month and 6 months
	EverX Flow, dentin shade	EXFD	1 week, 1 month and 6 months
	G-aenial Posterior	GP	1 week, 1 month and 6 months
Plain SFC (EXP or EXFD) 			
Bilayered specimens (n=60) Composed of SFC and PFC 	EverX Posterior covered with G-aenial Posterior	EXP-GP	1 week, 1 month and 6 months
	EverX Flow, dentin shade covered with G-aenial Posterior	EXFD-GP	1 week, 1 month and 6 months

PFC: particulate filler composite and SFC: short-fiber reinforced composite resin.

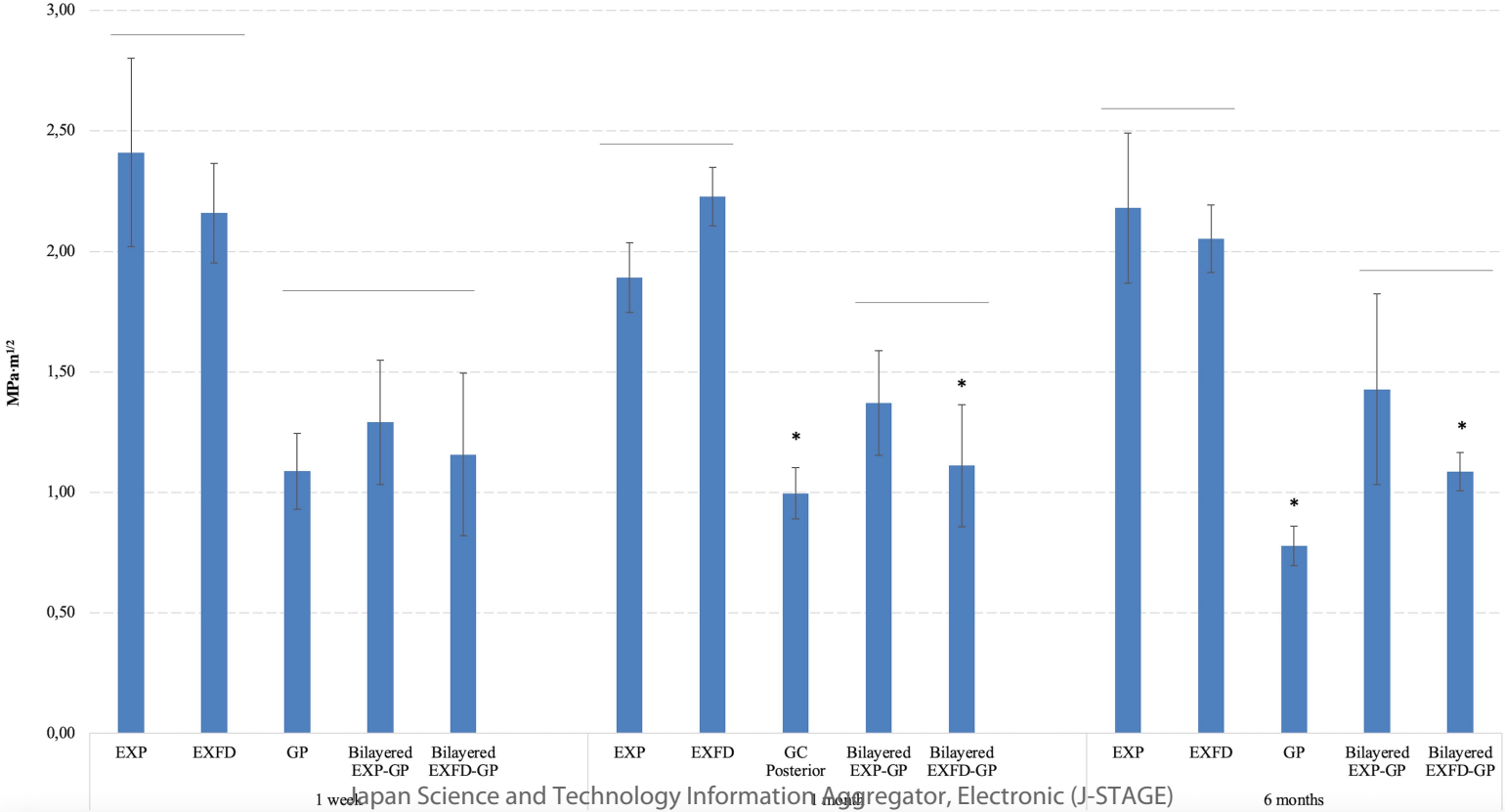
All specimens were stored in water at 37 degrees Celsius for 1 week, 1 month and 6 months.



Japan Science and Technology Information Aggregator, Electronic (J-STAGE)

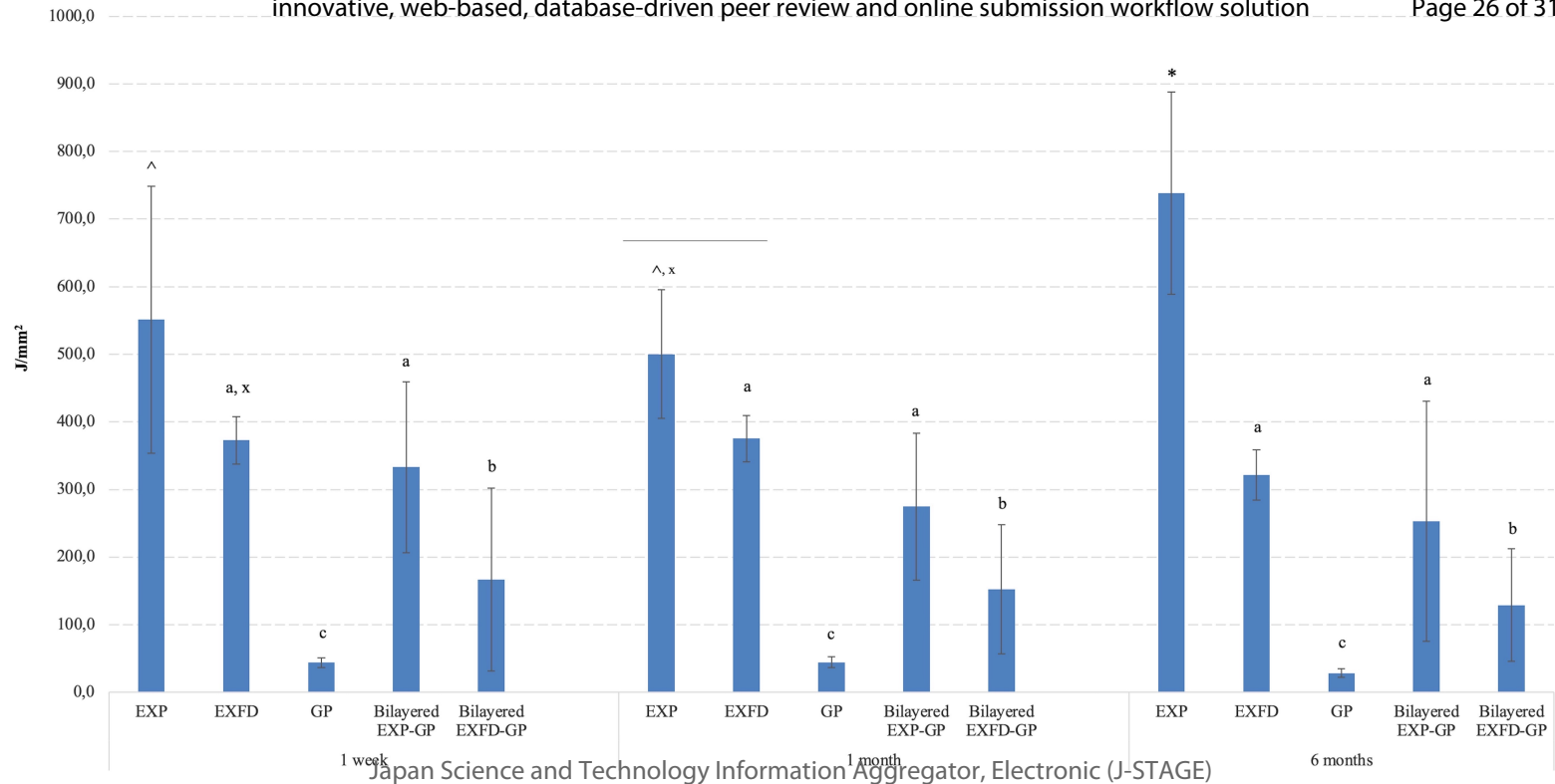
Fig. 1

The horizontal lines and the asterisk above the columns indicate statistically similar groups ($p > 0.05$)



Japan Science and Technology Information Aggregator, Electronic (J-STAGE)

Fig. 2



Japan Science and Technology Information Aggregator, Electronic (J-STAGE)

Fig. 3

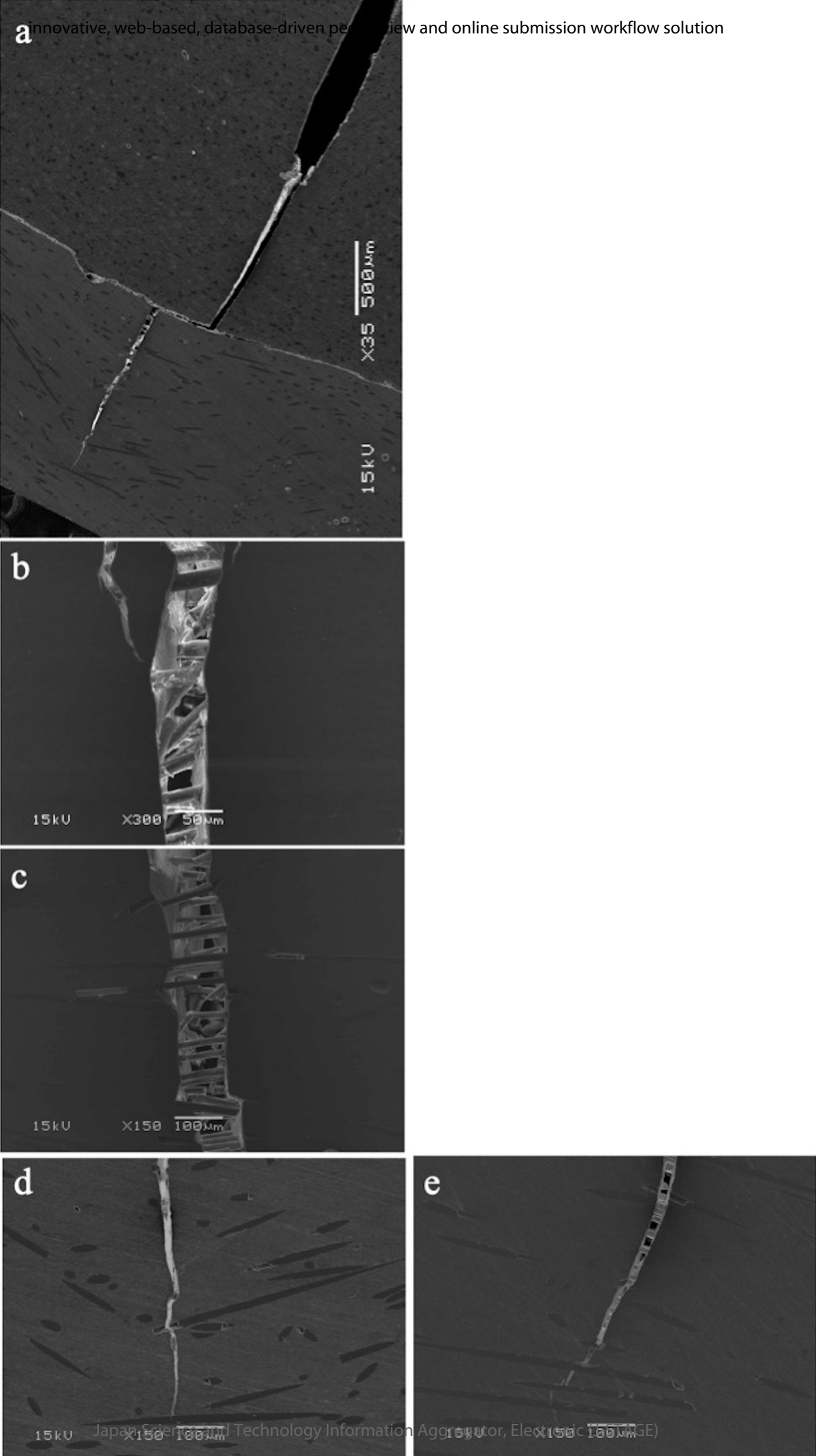


Fig. 4

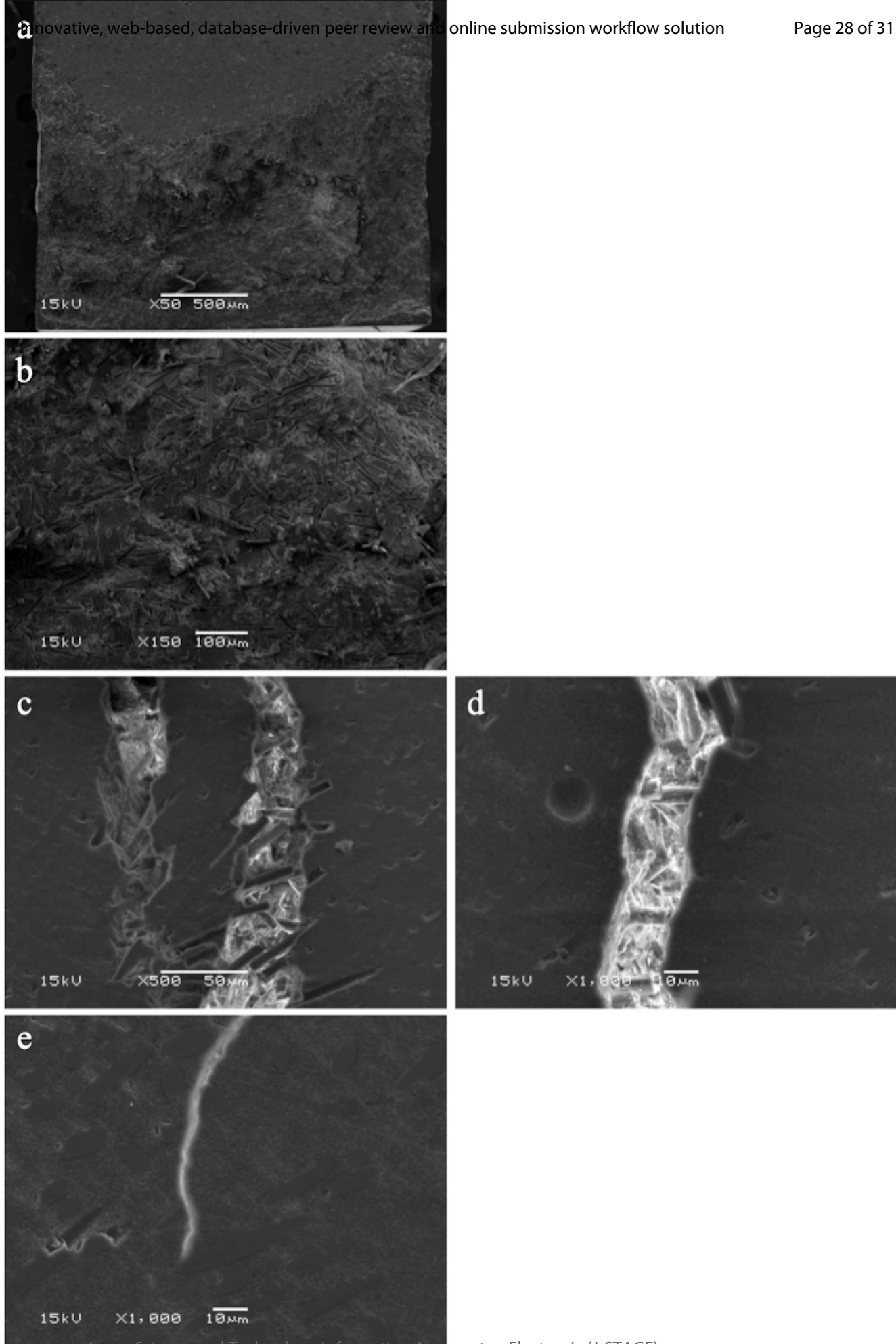


Fig. 5

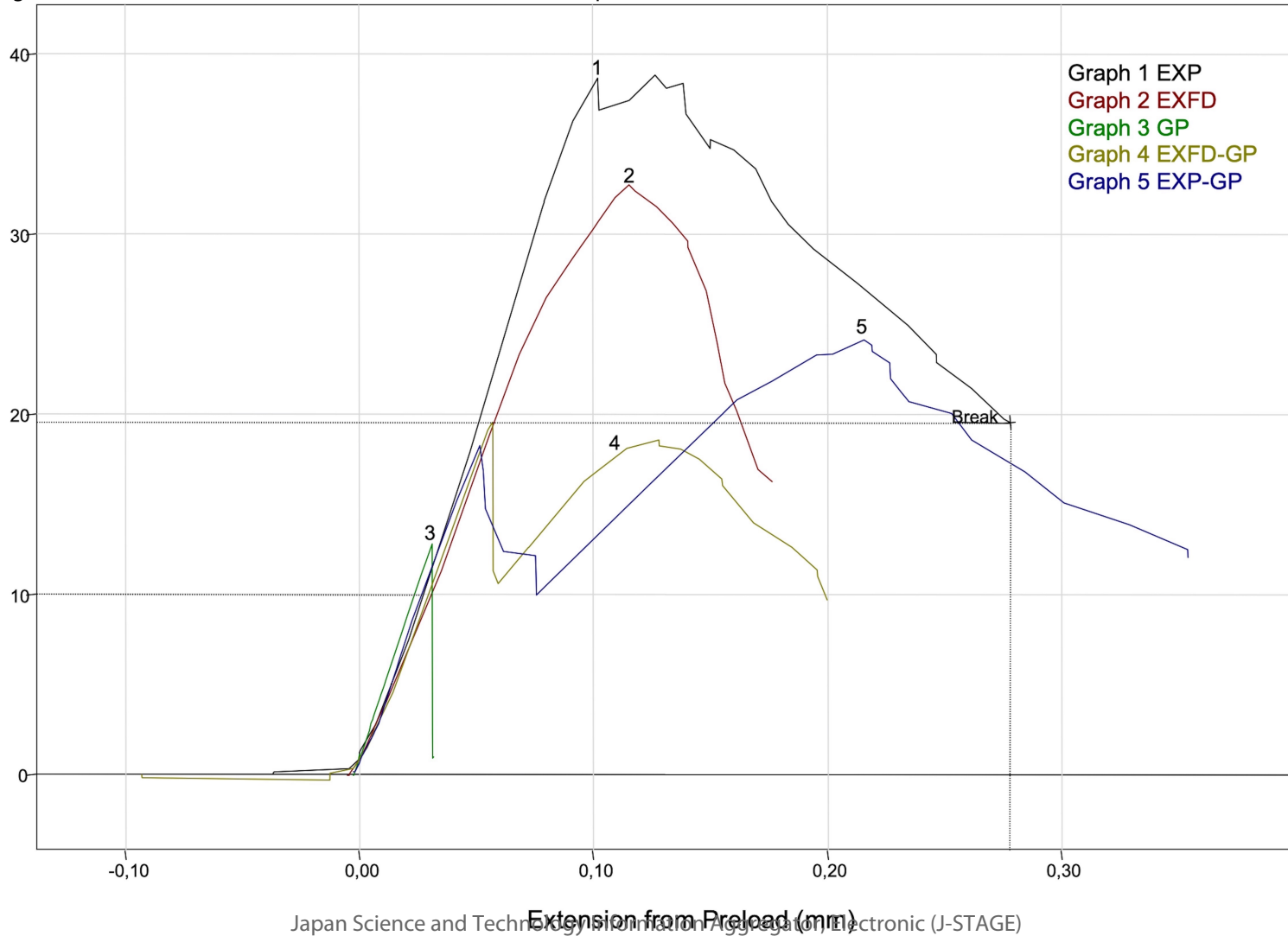
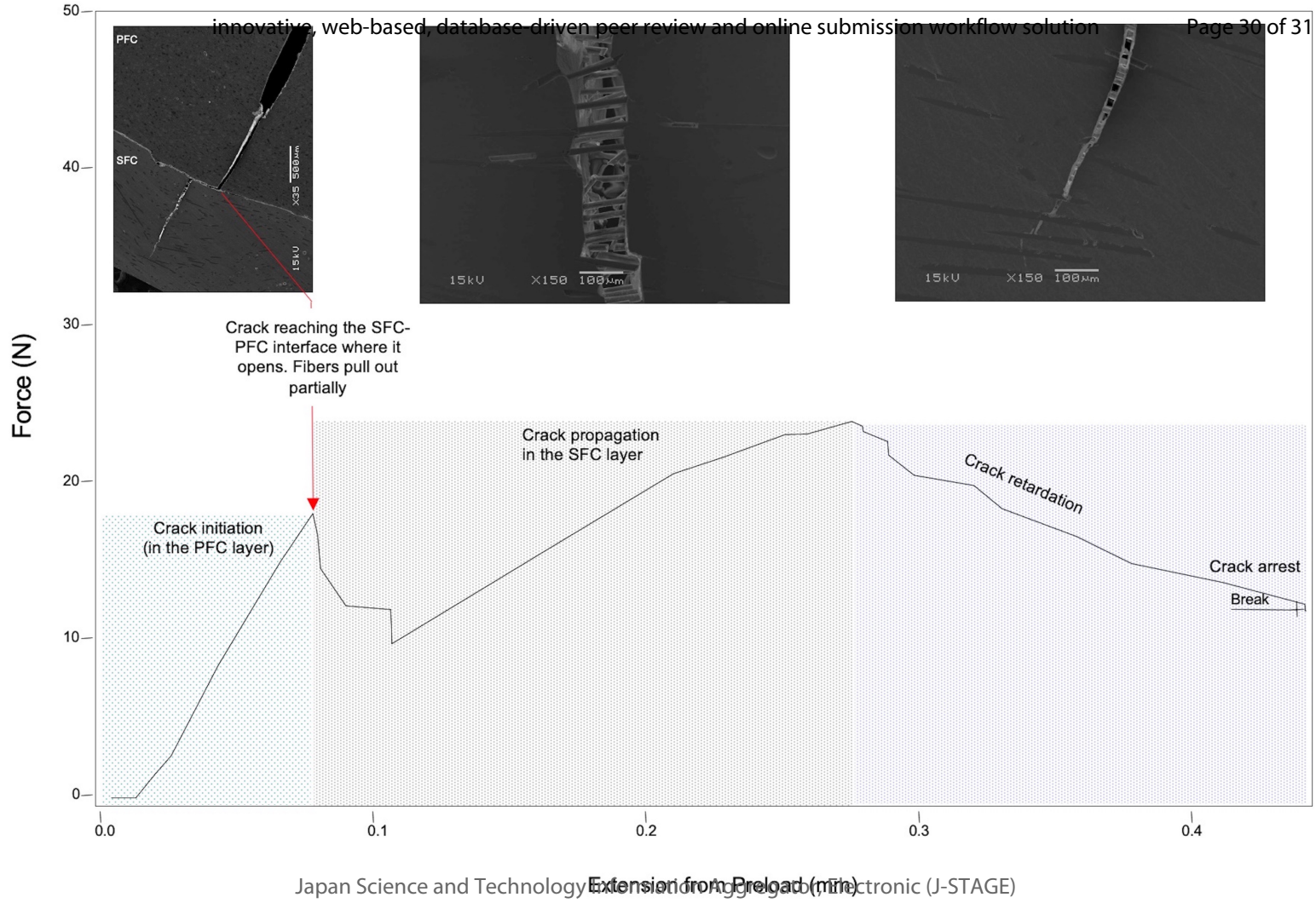


Fig. 6



Japan Science and Technology Agency (JST) and National Institute of Advanced Industrial Science and Technology (AIST) (J-STAGE)

Fig. 7a

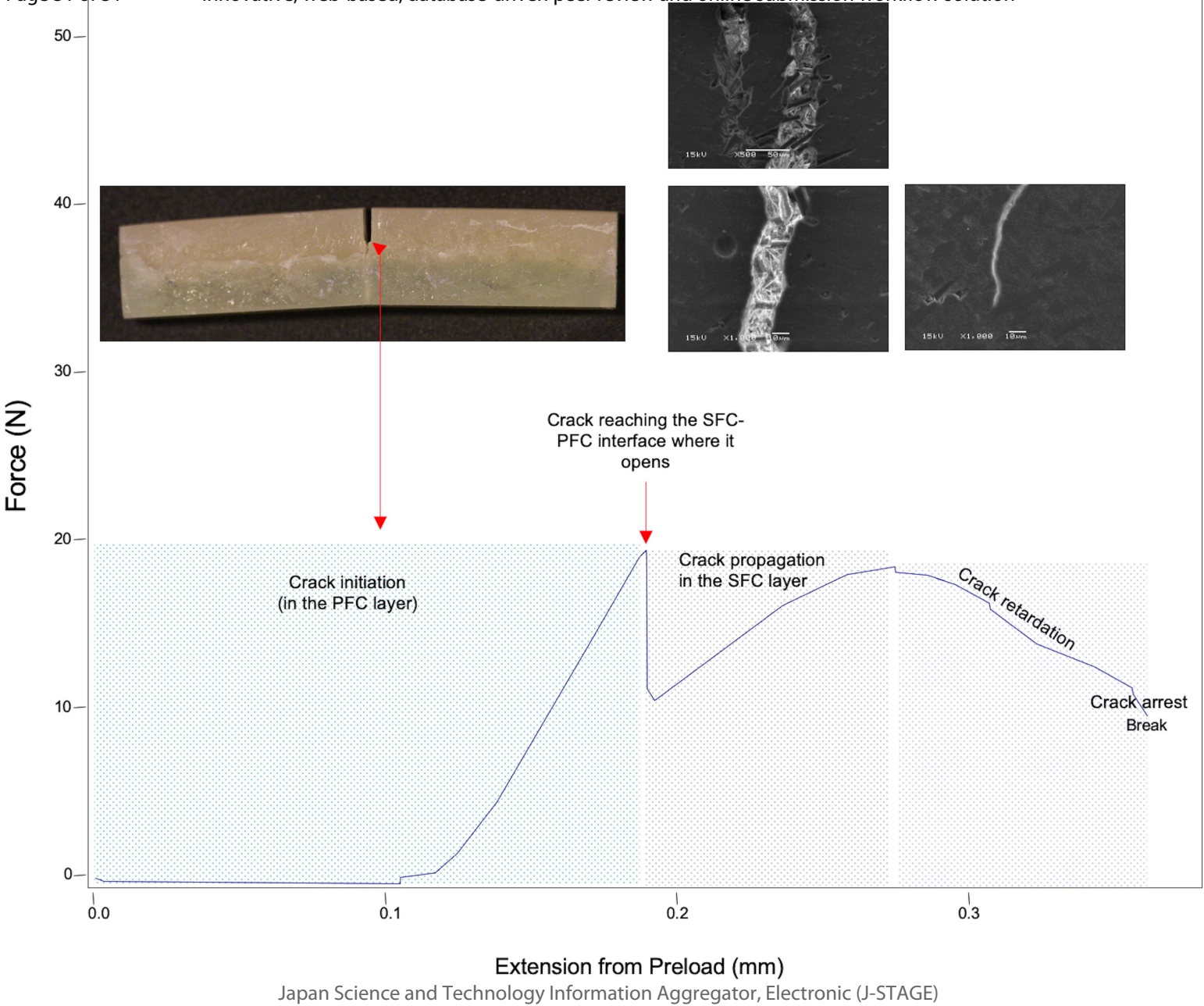


Fig. 7b